Computers and Electronics in Agriculture 167 (2019) 105093

Contents lists available at ScienceDirect

Computers and Electronics in Agriculture

journal homepage: www.elsevier.com/locate/compag

Crop conditional Convolutional Neural Networks for massive multi-crop plant disease classification over cell phone acquired images taken on real field conditions

Artzai Picon[a,*], Maximiliam Seitz[c,d], Aitor Alvarez-Gila[a], Patrick Mohnke[d], Amaia Ortiz-Barredo[b], Jone Echazarra[a]

[a] Computer Vision, TECNALIA, Parque Tecnolgico de Bizkaia, C/ Geldo. Edificio 700, E-48160 Derio, Bizkaia, Spain
[b] NEIKER, Plant health Dp, Arkaute Agrifood Campus, E-01080 Vitoria-Gasteiz, Araba, Spain
[c] Institute of Process Engineering in Plant Production, University of Hohenheim, 70599 Stuttgart, Germany
[d] BASF SE, Speyererstrasse 2, 67117 Limburgerhof, Germany

ARTICLE INFO

Keywords:
Convolutional neural network
Deep learning
Contextual meta-data
Contextual meta-data conditional neural network
Crop protection
Multi-label classification
Multi-crop classification
Image processing
Plant disease
Early pest
Disease identification
Precision agriculture
Phyto-pathology

ABSTRACT

Convolutional Neural Networks (CNN) have demonstrated their capabilities on the agronomical field, especially for plant visual symptoms assessment. As these models grow both in the number of training images and in the number of supported crops and diseases, there exist the dichotomy of (1) generating smaller models for specific crop or, (2) to generate a unique multi-crop model in a much more complex task (especially at early disease stages) but with the benefit of the entire multiple crop image dataset variability to enrich image feature description learning.

In this work we first introduce a challenging dataset of more than one hundred-thousand images taken by cell phone in real field wild conditions. This dataset contains almost equally distributed disease stages of seventeen diseases and five crops (wheat, barley, corn, rice and rape-seed) where several diseases can be present on the same picture.

When applying existing state of the art deep neural network methods to validate the two hypothesised approaches, we obtained a balanced accuracy ($BAC = 0.92$) when generating the smaller crop specific models and a balanced accuracy ($BAC = 0.93$) when generating a single multi-crop model.

In this work, we propose three different CNN architectures that incorporate contextual non-image meta-data such as crop information onto an image based Convolutional Neural Network. This combines the advantages of simultaneously learning from the entire multi-crop dataset while reducing the complexity of the disease classification tasks. The crop-conditional plant disease classification network that incorporates the contextual information by concatenation at the embedding vector level obtains a balanced accuracy of 0.98 improving all previous methods and removing 71% of the miss-classifications of the former methods.

1. Introduction

Plant pathogens; also causing fungal diseases; represent relevant biotic stress factors responsible for significant crop yield losses. Their damage potential is estimated among crops between 16 and 18% globally. The management of fungal diseases, which relays heavily on synthetic chemicals, can reduce pathogen caused potential yield losses by 32% (Oerke, 2006). To fully exploit this management potential, chemical crop protection treatments have to be applied based on infestation situation and time, which also maps the requirements of integrated crop protection. Therefore, continuous plant stock controls are required to identify disease symptoms in preferably early infestation stages to enable most efficient treatments. This is a time and cost intensive work (Kübler, 1994). In addition it can be assumed, that it is also challenging for common farmers as detailed knowledge of current pathogen species is necessary, especially for the visual identification of fungal disease symptoms at early infestation stages as similar stress symptoms are caused by different pathogens and abiotic factors (Oerke et al., 2010; Stafford, 2000).

Over the last few years, extensive research has been done on RGB image-based plant disease classification methods. Since the late 90s, classical computer vision approaches have been widely used to address

* Corresponding author.
E-mail address: artzai.picon@tecnalia.com (A. Picon).

https://doi.org/10.1016/j.compag.2019.105093
Received 21 May 2019; Received in revised form 24 September 2019; Accepted 3 November 2019
Available online 19 November 2019
0168-1699/

automated plant identification. Algorithms for wheat (Johannes et al., 2017; Xie et al., 2016; Siricharoen et al., 2016; Paul and Sharma, 2016; Barbedo, 2013; Wang et al., 2012), apple (Omrani et al., 2014), grape leaf (Sannakki et al., 2013; Meunkaewjinda et al., 2008), sugar beet (Zhou et al., 2013), tobacco (Guru et al., 2011), (soy bean Ahmad et al., 1999), (chili plant Husin et al., 2012), (cotton Gulhane and Gurjar, 2011; Gurjar and Gulhane, 2012), lemon tree (Pydipati et al., 2005; Pydipati et al., 2006) and areca nuts (Huang, 2012) among others have been developed.

A main handicap of classical computer vision methodologies that has been discussed by many authors (Shakoor et al., 2017; Kamilaris and Prenafeta-Boldú, 2018; Picon et al., 2018) is that they present a limited expressive power (Kamilaris and Prenafeta-Boldú, 2018). This keeps them away from further generalizing, thus laying on the bias extreme of the bias-variance trade-off, cannot take advantage of a larger number of training pictures and are not able to distinguish among diseases with subtle perceptual differences. Because of this, real field deployment of classical algorithms have always been difficult (Mohanty et al., 2016; Ferentinos, 2018; Picon et al., 2018) and image illumination normalization techniques were required to circumvent these limitations (Johannes et al., 2017).

The advent of Deep Convolutional Neural Networks (CNNs) has provided a flexible framework that allows for the definition of models that act both as descriptive hierarchical feature extractor and as classifier. CNN architectures can be extended and adapted in complexity to match the expressive power required by any given task and data availability. The agricultural field, and especially the image-based plant disease identification task, has not been an exception to this Kamilaris and Prenafeta-Boldú (2018). The seminal work carried out by Sladojevic et al. (2016) applied an AlexNet-like architecture (Krizhevsky et al., 2012) to model 13 different diseases from an image dataset obtained through internet online search. A huge effort was made on the generation of publicly available datasets with the PlantVillage initiative (Hughes et al., 2015). Their generated dataset contains more than 50,000 expertly curated images of healthy and infected leaves of 14 different crops (apple, blueberry, corn, grape, etc.) and a total number of 26 different diseases allowing their promoters to develop a disease identification classifier (Mohanty et al., 2016). Authors reported an accuracy of 99.35% on their model on a held-out test set. However, when the algorithm was tested under real field image conditions, the accuracy decreased to as low as 31.4%. The fact that only one type of disease is present at each image and that the images are taken under controlled conditions constitute the two main limitations that preclude its use as a real digital farming application where early disease detection on uncontrolled illumination conditions is essential for a correct deployment. Several studies have been conducted over this dataset: For example, Brahimi et al. (2018) analized the correspondence between the image saliency map and network activations to understand the behavior of the network obtaining state of art results, whereas Tan et al. (2018) restricted the PlantVillage dataset for a tomato-specific and detailed analysis. Deep learning networks have been also recently adapted to other crops such as rice (Alfarisy et al., 2018), grapevine (Cruz et al., 2018; Barré et al., 2018), wheat (Picon et al., 2018; Lu et al., 2017) or banana (Amara et al., 2017) and some recent work from (Ferentinos, 2018) used a dataset of more than 80,000 images to successfully distinguish among 58 distinct classes from 25 different crops with more than a 99% accuracy over the testing dataset by the use of five well-known CNN architectures.

Beside current advances, the disease classification problem is far from being solved. The extensive work from Barbedo (2016) analyzes its current challenges in deep detail. These challenges comprise:

1. The presence of multiple simultaneous disorders on a plant.
2. The existence of different disorders that present similar visual symptoms.
3. The high variability of symptoms for a specific disorder.
4. The complexity on the dataset acquisition, annotation and quality.

Table 1
Acquired and annotated image dataset.

Crop	EPPO-CODE	Disease Name	Disease EPPO-code	Total
Winter wheat	TRZAW	Abiotic	HEALTHY	6704
Winter wheat	TRZAW	Septoria tritici	SEPTTR	18,841
Winter wheat	TRZAW	Puccinia striiformis	PUCCST	15,376
Winter wheat	TRZAW	Puccinia recondita	PUCCRT	16,413
Winter wheat	TRZAW	Septoria nodorum	LEPTNO	602
Winter wheat	TRZAW	Drechslera tritici-repentis	PYRNTR	9550
Winter wheat	TRZAW	Oculimacula yallundae	PSDCHE	1489
Winter wheat	TRZAW	Gibberella zeae	GIBBZE	1207
Winter wheat	TRZAW	Blumeria graminis	ERYSGR	2866
			Total wheat:	64,026
Corn	ZEAMX	Abiotic	HEALTHY:	206
Corn	ZEAMX	Helminthosporium turcicum	SETOTU	425
			Total corn:	631
Rape seed	BRSNW	Abiotic	HEALTHY	6850
Rape seed	BRSNW	Phoma lingam	LEPTMA	6924
			Total rape seed:	13,774
Winter barley	HORVW	Abiotic	HEALTHY	1624
Winter barley	HORVW	Pyrenophora teres	PYRNTE	15,352
Winter barley	HORVW	Ramularia collo-cygni	RAMUCC	3441
Winter barley	HORVW	Rhynchosporium secalis	RHYNSE	11,279
Winter barley	HORVW	Puccinia hordei	PUCCHD	3323
			Total winter barley:	32,229
Common rice	ORYSA	Abiotic	HEALTHY	4051
Common rice	ORYSA	Various diseases	DIRTYP	206
Common rice	ORYSA	Thanatephorus cucumeris	RHIZSO	2438
Common rice	ORYSA	Pyricularia oryzae	PYRIOR	2441
			Total rice:	11,295
			Total:	121,955

The previously described approaches do not fully cover these challenges as they are focused on medium-late symptoms, do not cope with disorders with similar symptoms, do not support simultaneous diseases detection on the same plant and do not take advantage of additional information that could be included on the CNN topology to make the existing training dataset more efficient. As the existing CNN topologies from other fields have already demonstrated their capacity for plant disease identification, the agricultural research community is now paying more attention on their adaption and extension to solve the aforementioned plant disease classification-specific challenges. In this sense, Lu et al. (2017) proposed a MIL (Multiple Instance Learning) based approach over a fully convolutional network to integrate the neural network receptive field to focus on early disease activation map, whereas our recent work Picon et al. (2018) proposes a region-based method to focus on early diseases while allowing the detection of multiple diseases on the same plant.

It is also worth remarking that there is still no clear consensus on the necessity of creating specific network models for the identification of the diseases for each crop or if it is more efficient to create a single model capable of simultaneously identifying diseases for any of the analyzed plant species. The probability of the existence of different disorders with similar symptoms is greater, especially for early symptoms, when using a multi-crop model and this will increase the possibilities of miss-classifications. On the other hand, training a model over a larger dataset with higher variability will lead to learning richer and

Fig. 1. Examples of diseases images contained in the dataset for wheat (a) *Puccinia recondita*, (b) *Puccinia striiformis*, (c) *Drechslera tritici-repentis*, (d) *Septoria tritici*, (e) *Septoria nodorum*, (f) *Blumeria graminis*. On the top row the actual images on the dataset are depicted. On the bottom row, a magnified zoom of the diseased part is shown.

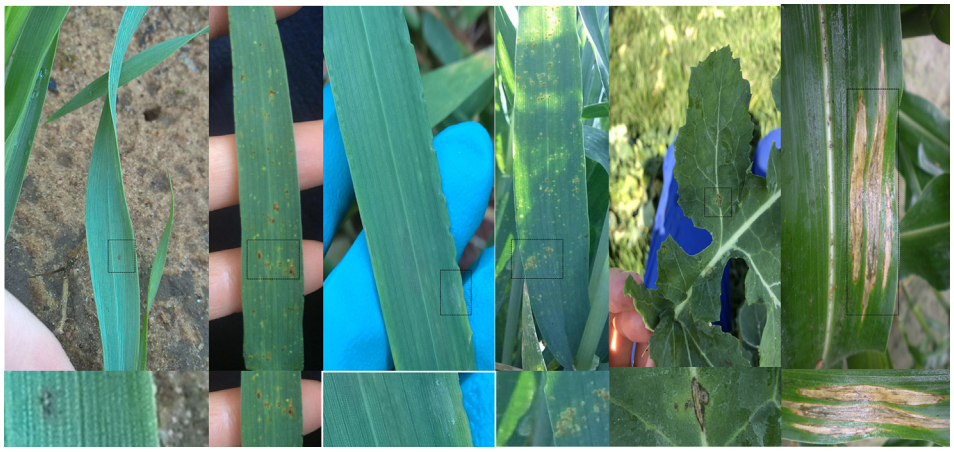

Fig. 2. Examples of diseases images contained in the dataset for barley: (a) *Pyrenophora teres*, (b) *Ramularia collo-cygni*, (c) *Rhynchosporium secalis*, (d) *Puccinia hordei*, rape seed: (e) *Phoma lingam*, corn: (f) *Helminthosporium turcicum*. On the top row the actual images on the dataset are depicted. On the bottom row, a magnified zoom of the diseased part is shown.

Fig. 3. Examples of diseases images contained in the dataset for barley: (a) *Phoma lingam (stem)*, wheat: (b) *Gibberella zeae (panicle)*, (c) *Oculimacula yallundae (stem)*, and rice: (d) *Pyricularia oryzae*, (e) Dirty panicle, (f) *Thanatephorus cucumeris*. On the top row the actual images on the dataset are depicted. On the bottom row, a magnified zoom of the diseased part is shown.

more robust visual features that are shared for all crops.

In order to focus on the aforementioned challenges, in this work we firstly introduce a challenging dataset of more than one hundred-thousand images taken by cell phone in real field wild conditions that contains almost equally distributed disease stages of seventeen diseases and five crops (wheat, barley, corn, rice and rape-seed) where several diseases can be present on the same picture, present high visual variability and different diseases present similar visual symptoms which is introduced in Section 2.

We propose a CNN architecture that is able to seamlessly incorporate contextual meta-data, such as the plant species information, which allows training a single multi-crop model that: (a) obtains richer and more robust shared visual features than the single crop counterparts and (b) does not suffer from the presence of different disorders with similar symptoms from the different crops and (c) seamlessly integrates contextual meta-data to perform crop-conditional disease classification. These topologies are detailed in Section 3.2 and results are discussed on Section 4. Section 5 summarizes the conclusions of this work.

The experiments carried out in this work lead to the validation of the following hypothesis:

1. Applying existing CNN topologies for a multi-crop disease identification task trained by a complete multi-crop dataset where different disorders with similar symptoms are present reduces the overall performance of the trained model due to task increased complexity.
2. The generation of separate classification models for each crop do not take advantage of the information from other crops specially for crops and/or diseases with a low number of images.
3. The use of an extended CNN topology integrating plant species information as complementary information to the input image over a complete multi-crop dataset surpasses the performance obtained by the two first methods taking advantage on the visual information and variability from the full dataset and not suffering from the effect of diseases with similar appearance from other crops.

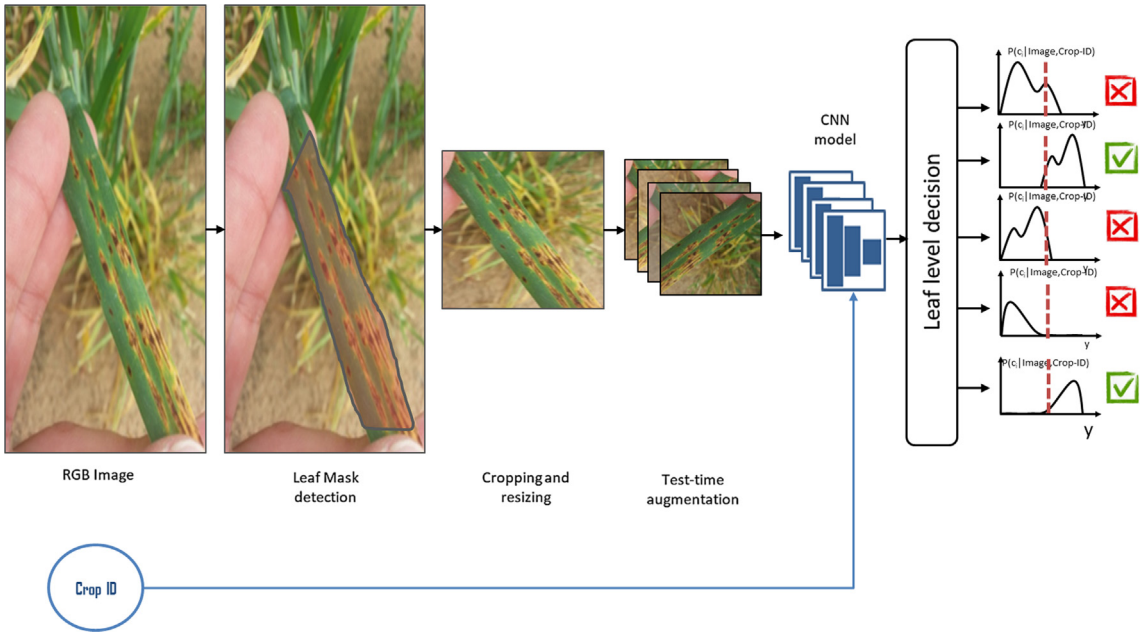

Fig. 4. Crop conditional disease classification pipeline.

2. Material & methods

2.1. Extensive, multi-crop and wide field conditions dataset

In this section we introduce the challenging dataset that has been generated as a testbed for focusing on the plant disease challenged summarized by Barbedo (2016). To this end, we have generated a dataset of more than one hundred-thousand images taken by cell phone in real field wild conditions that contains almost equally distributed disease stages of seventeen diseases and five crops (wheat, barley, corn, rice and rape-seed) that have been taken on the field. Due to the nature of disease spreading in plants, several diseases can be present on the same plant. Some of the targeted diseases have been selected as they present similar visual symptoms between them adding more complexity to the dataset. Finally, diseases from leaves, stem and panicle have been included. For the presented work, the wheat dataset used at Picon et al. (2018) containing 8178 field images have been extended. This dataset included Septoria (*Septoria triciti*), Tan Spot (*Drechslera triciti-repentis*) and Rust (*Puccinia striiformis, Puccinia recondita*) diseases over more than 36 wheat plant varieties. Four new crops have been added to the existing winter wheat (*Triticum aestivum*) species: corn (*Zea mays*), rape seed (*Brassica napus*), winter barley (*Hordeum vulgare*) and common rice (*Oryza sativa*).

The number of winter wheat diseases have been extended including eight different diseases (*Septoria tritici*, *Puccinia striiformis*, *Puccinia recondita*, *Septoria nodorum*, *Drechslera tritici-repentis*, *Gibberella zeae*, *Blumeria graminis* and *Oculimacula yallundae*). For corn, the *Helminthosporium turcicum* disease have been included in the database, whereas rape seed crop includes *Phoma lingam* disease, winter barley crop includes four different diseases: *Pyrenophora teres*,*Ramularia collo-cygni*,*Rhynchosporium secalis* and *Puccinia hordei*. Common rice crop includes three diseases: *Thanatephorus cucumeris*, *Pyricularia oryzae* and dirty panicle (which is caused by multiple fungal species). The entire dataset comprises a total number of 121,955 images, as shown in Table 1. The new dataset includes now diseases that appears not only over the leaf, but also on the stem and panicle of the plant and several diseases might appear on the same image.

For an optimal pest control, diseases need to be detected at the early stages of symptoms' development, so as to assure appropriate and efficient measures adapted to the stage of the infection. Because of this, the generated dataset contains images at different stages of infection. Approximately, 25% of the images belong to initial stages of the infection, 25% to early stages, 25% to medium stages and 25% to advanced stages. This generates a highly complex dataset where, especially for early symptoms, different diseases produced similar or slightly different symptoms that are difficult to cope with using common algorithms. Examples of pictures in the dataset are presented in Figs. 1–3.

It is noteworthy to state that this dataset includes diseases that generate very similar symptoms, especially on early stages and that more than one disease might be present on the same leaf. In this sense, before the typical visual appearance of a disease occurs, a very common effect is that the leaves show different shapes of chloroses. This is true not only for biotic stress, but also for abiotic stress, which complicates the exact determination of the disease further. For example, the initial symptoms in Wheat of *Puccinia recondita* and *Puccinia striiformis* and also in Barley of *Ramularia collo-cygni* and *Puccinia hordei* show very similar chloroses, as seen in Fig. 1 and 2 brightening of small patches with slight differences in color and shape. When the typical cluster of spores on the chloroses occurs, the curative treatment is mostly too late, which underlines the difficulty and importance of the early detection. In addition, there are also diseases where not only the early infestation are quite similar but also the advanced stages are difficult to distinguish. Regarding *Septoria tritici* and *Septoria nodorum*, both have analogous disease progressions. First chloroses can be seen, which evolve to necroses and, in the end, brown or black pycnidia occur on the necroses.

The pictures were acquired trying to get an appropiate focus with the flash mode of the camera set to off. No other limitations were imposed to the technicians to simulate real field acquisition conditions. The use of additional normalization color elements was avoided as they are unpractical for field image acquisition, as shown in Johannes et al. (2017). All new images were cropped to the region surrounding their main leaf, following the *Leaf-mask crop* approach proposed in Picon et al. (2018). To do this, the main leaf, stem or panicle at each image was automatically segmented by a fully convolutional DenseNet network (Jégou et al., 2017) where the pixel-wise categorical cross-entropy loss function was complemented with a total variation term Chambolle (2004),Bereciartua et al. (2015) that penalizes the segmentation of irregular regions. Each image was also labeled with all the diseases that are presented in a multi-label scheme where an image can

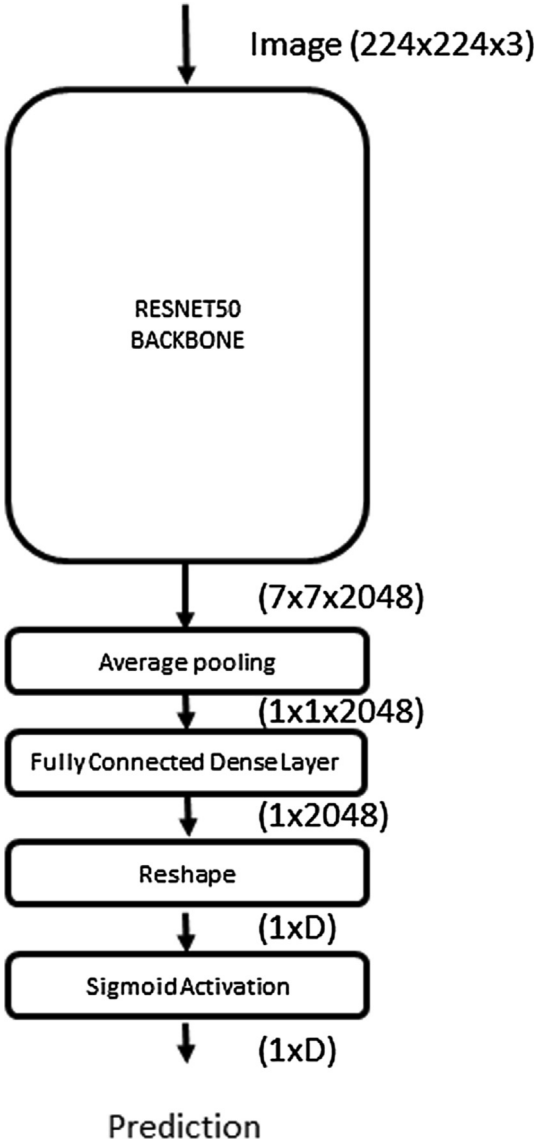

Fig. 5. Baseline ResNet50 Architecture.

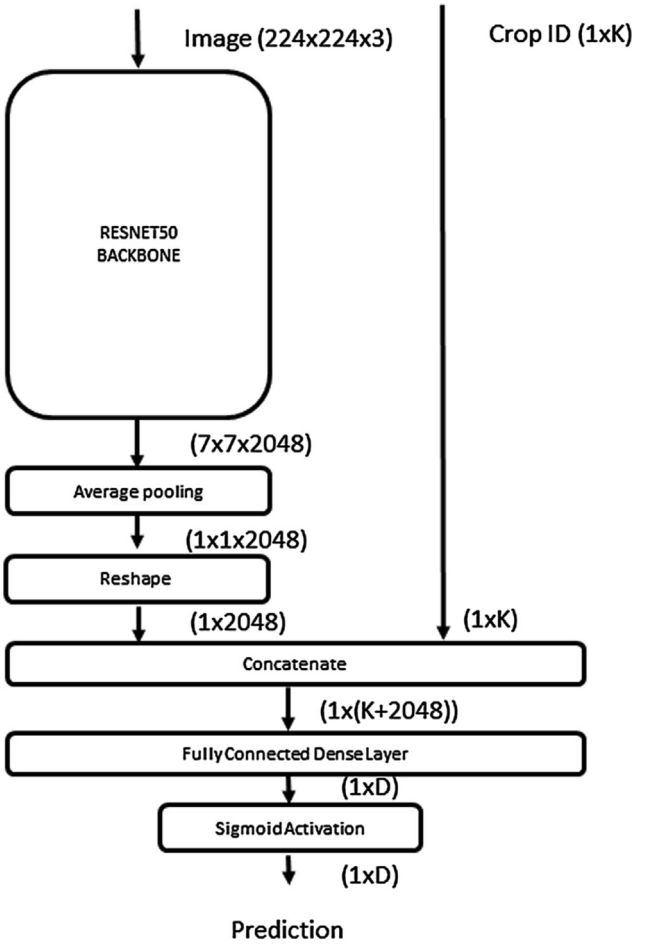

Fig. 6. Topology for multi-crop network with crop information aggregation by high level feature extraction layer concatenation.

have multiple diseases. New images containing diseases located at stem or panicle were manually segmented following the manual procedure described in Picon et al. (2018).

3. Convolutional Neural Network for disease classification

In this section, we introduce three different convolutional neural network (CNN) architectures that combines categorical metadata (such as crop identification, weather conditions, geographical location,…) within a image based convolutional neural network. Fig. 4 shows the overall pipeline: A RGB image is taken by a mobile device. Leaf, stem or panicle is detected and the image is cropped and resized to the leaf bounding box. Obtained images are then visually augmented and feed a convolutional neural network following one of the architectures described on this section.The output of the network with the different augmentations is averaged. Crop ID information is also fed into the convolutional neural network to include the contextual categorical metadata on the proposed crop conditional CNN architecture.

Network final layer is based on a fully connected layer of a number of output neurons corresponding to the number of total diseases. The use of a *sigmoid* activation function makes the last layer outputs independent. This means that each neuron can be activated on the presence of its corresponding disease regardless the activation of the other neurons.

3.1. Baseline architecture (ResNet50)

We propose a baseline network that only use image information for disease classification and have shown excellent performance when detecting early diseases Picon et al. (2018). This network is derived from the *ResNet50* topology presented by He et al. (2016).This network architecture was selected based on the desire of a widely used network with state of the art performance. However, the proposed crop conditional approach is also valid with other baseline topologies such as VGG (Simonyan and Zisserman, 2014), DenseNet (Huang et al., 2017) or Inception (Szegedy et al., 2016).

This network is composed of 50 layers with two consecutive 3×3 convolutions, followed by 3×3 max-pooling operations. This is followed by a set of consecutive residual blocks that gradually reduce the size of the activations in the spatial domain while growing on the feature domain, yielding an image representation that comprise $7x7x2048$ high level features that are finally integrated by an *average pooling* operation to finally get a *image representation layer* consisting of 2048 features. This *back-bone* topology is followed by a dense layer with an output size equal to the number D of the disease classes followed by a *sigmoid* activation. The use of the *sigmoid* function instead of the *softmax* enabled the detection of multiple diseases on the same leaf as it allows the independent activation of the last layer neurons, while at the same time allowing sharing the weights by means of a common disease feature description. This network topology is depicted in Fig. 5 and a

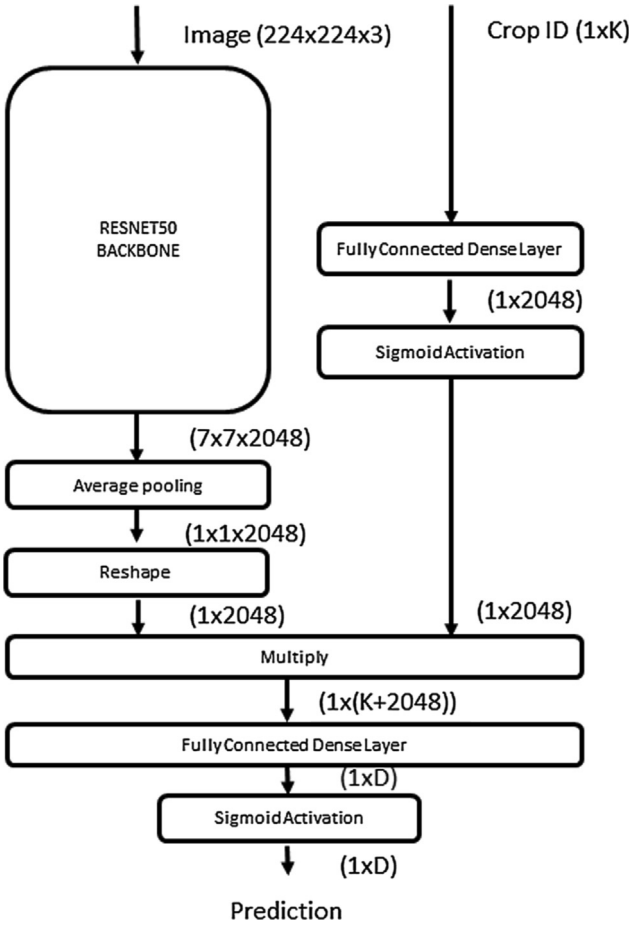

Fig. 7. Topology for multi-crop network with crop information aggregation by high level feature extraction multiplicative suppression.

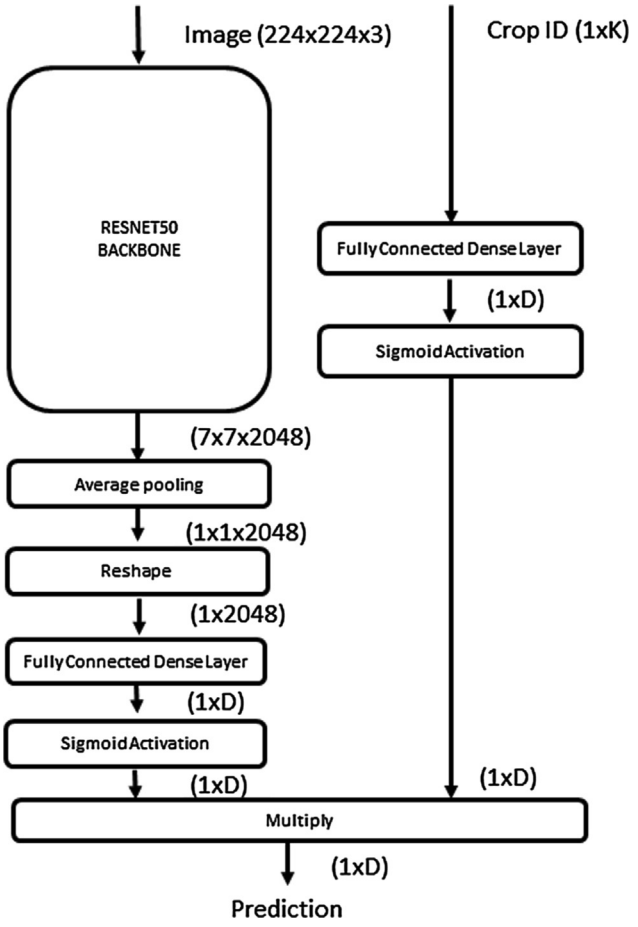

Fig. 8. Topology for multi-crop network with crop information aggregation by classification layer multiplicative suppression.

more detailed description can be found at Picon et al. (2018).

3.2. Crop Conditional Convolutional Neural Network for disease classification

The use of complementary additional contextual meta-data has been widely used in image analysis to guide the classifier response for improving its performance for specific domains. For example, camera meta-data have been used to complement information to get accurate semantic scene classification Boutell and Luo (2005, 2004), geo-spatial position has been used by Chen et al. (2011) to improve landmark identification from mobile devices, past user behaviour serves to predict its current actions (Picón et al., 2012) or the use conditional generative models can serve to produce a synthetic image from the requested class (Mirza and Osindero, 2014).

In the crop protection domain, this additional information is already being provided independently to generate pathogen risk maps based on weather and satellite models Venette et al. (2010),Magarey et al. (2007) that can be complementary the visual information collected on the field by mobile applications to create more elaborated and precise statistical models. However, most of the existing deep learning-based architectures for image classification only rely on the visual image information to perform a prediction without any additional consideration. Apart from weather conditions or pathogen risk map, one of the main prior information that can support disease detection is the knowledge of the crop we are analyzing, which is already known by the farmer.

We propose three different approaches to seamlessly integrate contextual meta-data to complement the image information that serves as input for the classification system with the additional information of the crop (plant species) that is present on the taken image by extending the baseline convolutional neural network architecture described in Section 3.

3.2.1. Concatenation of crop information at feature extraction layer (RESNET-MC-1)

We represent crop information as a categorical vector of K components where K is the number of crops in the model. This vector has value 1 at the component corresponding to its crop class and value 0 for the other components.

On this proposed topology, depicted in Fig. 6, the crop vector is directly aggregated by a concatenation layer into the *image representation layer* or image embeddings layer. This yields a joint activation that combines the image descriptive features from the image representation layer with the information of the plant species (crop) that is present on the picture. A subsequent fully connected layer is responsible of mapping the relationships between the image high level features and the crop with the disease predictions.

During the end-to-end training process, both the visual feature representation at the image representation layer and the subsequent crop-disease mapping are jointly learned. Intuitively, the learned visual features that are shared by all crops deal to a richer dataset representation.

3.2.2. Multiplicative suppression of the feature extraction layer activations (RESNET-MC-2)

The second proposed topology, that is depicted in Fig. 7, follows a different motivation. In this case, the crop vector is not concatenated as

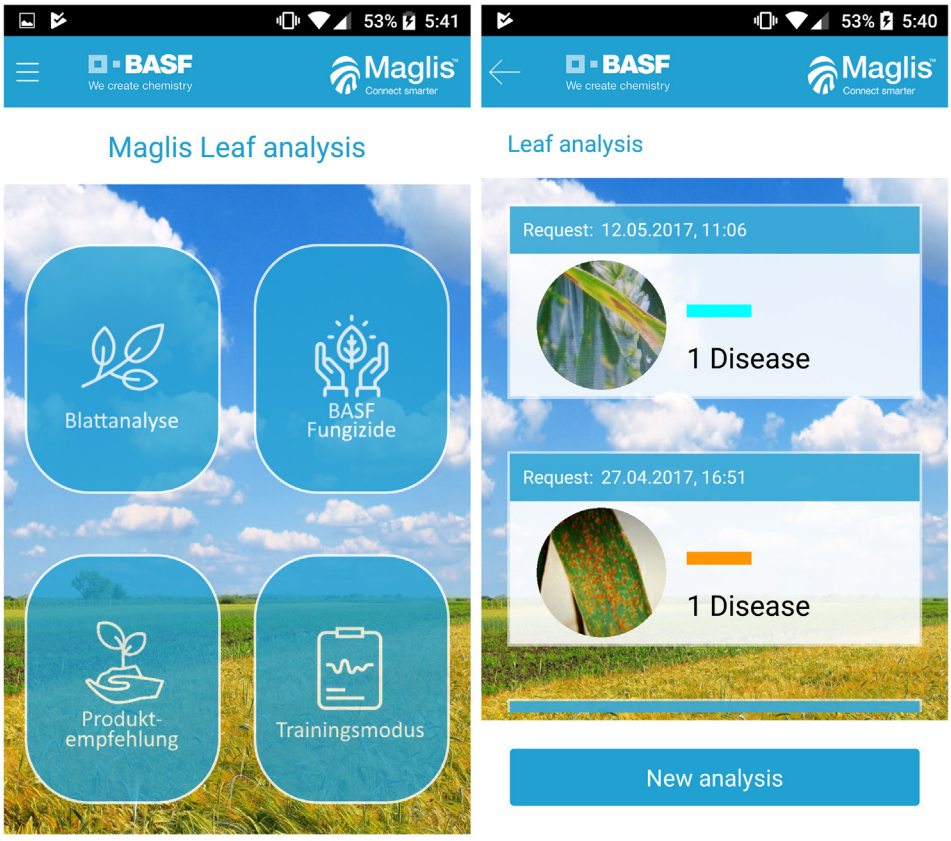

Fig. 9. Developed mobile application for disease identification.

Table 2
Results for baseline topology ResNet50 with crops trained separately over the testing set.

Network Topology	ResNet50	Training dataset	SEPARATED-CROPS			
Disease	AuC	BAC	Sens	Spec	NPV	PPV
SEPTTR	0.95	0.88	0.87	0.89	0.94	0.77
PUCCST	0.98	0.93	0.91	0.95	0.97	0.86
PUCCRT	0.95	0.87	0.81	0.93	0.93	0.80
LEPTNO	0.97	0.82	0.65	0.99	1.00	0.44
PYRNTR	0.96	0.87	0.76	0.98	0.96	0.85
PSDCHE	1.00	0.99	0.99	1.00	1.00	0.99
GIBBZE	1.00	0.99	0.98	1.00	1.00	0.96
ERYSGR	1.00	0.98	0.96	1.00	0.92	0.90
SETOTU	0.91	0.76	0.93	0.58	0.79	0.84
LEPTMA	1.00	1.00	1.00	1.00	1.00	1.00
PYRNTE	0.96	0.91	0.87	0.94	0.89	0.93
RAMUCC	1.00	0.95	0.90	0.99	0.99	0.95
RHYNSE	0.99	0.96	0.95	0.97	0.97	0.95
PUCCHD	0.99	0.92	0.85	0.99	0.98	0.91
DIRTYP	0.99	0.94	0.94	0.95	0.98	0.83
RHIZSO	1.00	0.99	0.98	0.99	1.00	0.97
PYRIOR	1.00	0.97	0.95	1.00	0.99	0.98

Table 3
Results for baseline topology ResNet50 with all crops trained together over the testing set.

Network Topology	ResNet50	Training dataset	ALL-CROPS			
Disease	AuC	BAC	Sens	Spec	NPV	PPV
SEPTTR	0.98	0.90	0.83	0.96	0.97	0.81
PUCCST	0.99	0.94	0.90	0.99	0.98	0.92
PUCCRT	0.98	0.89	0.82	0.97	0.97	0.80
LEPTNO	0.98	0.79	0.59	1.00	1.00	0.50
PYRNTR	0.98	0.89	0.80	0.98	0.98	0.82
PSDCHE	1.00	0.99	0.99	1.00	1.00	0.99
GIBBZE	1.00	0.99	0.97	1.00	1.00	0.99
ERYSGR	1.00	0.97	0.94	1.00	1.00	0.90
SETOTU	1.00	0.96	0.91	1.00	1.00	0.93
LEPTMA	1.00	0.99	1.00	1.00	1.00	0.98
PYRNTE	0.99	0.91	0.84	0.99	0.98	0.90
RAMUCC	1.00	0.95	0.90	1.00	1.00	0.94
RHYNSE	0.99	0.95	0.92	0.99	0.99	0.93
PUCCHD	0.99	0.87	0.74	1.00	0.99	0.82
DIRTYP	1.00	0.97	0.94	1.00	1.00	0.81
RHIZSO	1.00	0.96	0.92	1.00	1.00	0.95
PYRIOR	1.00	0.96	0.92	1.00	1.00	0.96

an additional feature as in the previous topology, but it is instead used to suppress the activation of certain visual features when they are irrelevant for the plant species that is present on the image.

In this case, the crop vector is directly connected to a fully connected dense layer with 2048 neurons that correspond with the number of features at the *image representation layer*. The resulting signal is then connected to a sigmoid activation function that maps the output into the [0,1] range. The integration of this signal with the *image representation layer* is performed by an element-wise multiplication layer. In this way, the plant species that is present on the image modulates the response of the learned visual descriptors that are learnt within the training procedure, thus reducing the effect of the learnt visual features that are inconsistent to the provided context (crop identification information).

3.2.3. Multiplicative suppression of inconsistent predictions (RESNET-MC-3)

The third proposed topology, depicted in Fig. 8, replicates the multiplicative suppression of the activations. However, in this case, the multiplicative suppression is performed at higher abstraction level, directly over the final predictions of the network, just suppressing the activation of the neurons that are mapping the disease presence. This

Table 4
Results with RESNET-MC-1 architecture over the testing set.

Network Topology	RESNET-MC-1	Training dataset	ALL-CROPS			
Disease	AuC	BAC	Sens	Spec	NPV	PPV
SEPTTR	1.00	0.96	0.94	0.98	0.99	0.92
PUCCST	1.00	0.98	0.97	1.00	0.99	0.97
PUCCRT	1.00	0.95	0.91	0.99	0.99	0.92
LEPTNO	1.00	0.94	0.88	1.00	1.00	0.86
PYRNTR	1.00	0.96	0.92	0.99	0.99	0.90
PSDCHE	1.00	0.99	0.99	1.00	1.00	0.97
GIBBZE	1.00	1.00	0.99	1.00	1.00	0.96
ERYSGR	1.00	0.99	0.99	1.00	1.00	0.92
SETOTU	1.00	0.98	0.96	1.00	1.00	1.00
LEPTMA	1.00	0.99	0.98	1.00	1.00	1.00
PYRNTE	1.00	0.97	0.95	0.99	0.99	0.94
RAMUCC	1.00	0.99	0.98	1.00	1.00	0.95
RHYNSE	1.00	0.98	0.97	1.00	1.00	0.98
PUCCHD	1.00	0.98	0.96	1.00	1.00	0.89
DIRTYP	1.00	0.97	0.95	1.00	1.00	0.86
RHIZSO	1.00	0.99	0.97	1.00	1.00	0.98
PYRIOR	1.00	0.98	0.97	1.00	1.00	0.98

Table 5
Results with RESNET-MC-2 architecture over the testing set.

Network Topology	RESNET-MC-2	Training dataset	ALL-CROPS			
Disease	AuC	BAC	Sens	Spec	NPV	PPV
SEPTTR	0.97	0.88	0.81	0.96	0.96	0.77
PUCCST	0.99	0.93	0.88	0.99	0.98	0.90
PUCCRT	0.97	0.88	0.79	0.97	0.97	0.79
LEPTNO	0.98	0.77	0.55	1.00	1.00	0.39
PYRNTR	0.98	0.88	0.77	0.99	0.98	0.82
PSDCHE	1.00	0.99	0.99	1.00	1.00	0.99
GIBBZE	1.00	0.99	0.97	1.00	1.00	0.96
ERYSGR	1.00	0.95	0.90	1.00	1.00	0.84
SETOTU	1.00	0.97	0.93	1.00	1.00	0.89
LEPTMA	1.00	0.99	0.97	1.00	1.00	0.99
PYRNTE	0.99	0.91	0.82	0.99	0.98	0.91
RAMUCC	1.00	0.96	0.92	1.00	1.00	0.89
RHYNSE	0.99	0.94	0.88	0.99	0.99	0.94
PUCCHD	0.99	0.86	0.73	1.00	0.99	0.82
DIRTYP	1.00	0.99	0.99	0.99	1.00	0.77
RHIZSO	1.00	0.94	0.88	1.00	1.00	0.93
PYRIOR	1.00	0.95	0.90	1.00	1.00	0.96

Table 6
Results with RESNET-MC-3 architecture over the testing set.

Network Topology	RESNET-MC-3	Training dataset	ALL-CROPS			
Disease	AuC	BAC	Sens	Spec	NPV	PPV
SEPTTR	0.97	0.89	0.82	0.95	0.97	0.77
PUCCST	0.99	0.93	0.87	0.98	0.98	0.88
PUCCRT	0.97	0.88	0.81	0.95	0.97	0.73
LEPTNO	0.98	0.79	0.59	1.00	1.00	0.40
PYRNTR	0.98	0.89	0.81	0.98	0.98	0.77
PSDCHE	1.00	0.99	0.99	1.00	1.00	0.95
GIBBZE	1.00	0.99	0.97	1.00	1.00	0.98
ERYSGR	1.00	0.94	0.87	1.00	1.00	0.88
SETOTU	1.00	0.99	0.98	1.00	1.00	0.79
LEPTMA	1.00	0.98	0.95	1.00	1.00	0.99
PYRNTE	0.99	0.91	0.82	0.99	0.98	0.90
RAMUCC	1.00	0.94	0.88	1.00	1.00	0.92
RHYNSE	0.99	0.94	0.90	0.99	0.99	0.90
PUCCHD	0.99	0.87	0.74	1.00	0.99	0.73
DIRTYP	1.00	0.98	0.98	0.99	1.00	0.75
RHIZSO	1.00	0.98	0.96	1.00	1.00	0.86
PYRIOR	1.00	0.96	0.92	1.00	1.00	0.94

Table 7
Performance metrics for the different architectures.

Architecture	AuC	BAC	Sens	Spec	NPV	PPV
Single-Crop	0.98	0.93	0.90	0.95	0.96	0.88
Multi-Crop	0.99	0.93	0.88	0.99	0.99	0.88
Conditional MC1	**1.00**	**0.98**	**0.96**	**1.00**	**1.00**	**0.94**
Conditional MC2	0.99	0.93	0.86	0.99	0.99	0.86
Conditional MC3	0.99	0.93	0.87	0.99	0.99	0.83

models inconsistencies of the presence of diseases that should not exist on the specific targeted represented plant-specie.

4. Results

4.1. Training procedure

A training database was created from the dataset defined in Table 1. In order to avoid bias, the dataset was divided into 80% of the images for training, another 10% for validation and a final 10% for the testing set. All results are provided over the testing set. Picture acquisition date was set as division criterion to avoid pictures taken the same day to belong to different sets. The Area under the Receiver Operating Characteristic (ROC) Curve (AuC) shows overall algorithm performance metric. Computed values of sensitivity, specificity and balanced accuracy (BAC), Negative predictive value (NPV) and positive predictive value (PPV) for the different diseases are also provided for the threshold value that maximizes the validation set accuracy, following the same methodology used at Johannes et al. (2017) and at Picon et al. (2018).

During the training process, we followed the same training pipeline and data augmentation scheme as proposed at Picon et al. (2018), where the process is described in detail:

- On the first stage, the main trunk of the network architecture (as described in Section 3.1) is pre-trained over the Imagenet dataset Russakovsky et al. (2015). This pre-trained network serves as a backbone network for testing the different network topologies.
- On the second stage, each network topology proposed in Section 3.2 is loaded with the pre-trained weights for all the shared layers and their weights are kept frozen. The last dense layer and the layers corresponding to the integration of the crop identification information are randomly initialized, and these are the only ones allowed to modify their weights during learning at this stage.
- The final training stage completes the fine-tuning by starting from the weights resulting from the previous stage and unfreezing all the layers, thus yielding a free, unconstrained training.

The network was trained using Stochastic Gradient Descent (SGD) optimization with an initial learning rate of 10^{-4}, a learning rate decay of 10^{-6} and a momentum of 0.9. For the second training stage, the network was first trained during 10 epochs while keeping the rest frozen, and afterwards the full network was trained.

Tensorflow/Keras framework over python 3.7 was used to implement the proposed network architectures. Models where trained on a Ubuntu 16.04 server with four 16 GB memory Tesla V100-DGXS-16 GB GPU cards. Each of the experiments took 1–2 weeks for training. Deployment computational time of the developed network including test time augmentation is 200 ms per image with just CPU acceleration. Deployment model was encapsulated into a docker container with an secured and authenticated REST service to allow connection with the mobile application depicted on Fig. 9.

4.2. Image based Convolutional Neural Network

In this section we analyze the results of the image based

Convolutional Neural Network (CNN) without the inclusion of any contextual metadata to serve as a baseline model that takes into consideration only the given image and does not integrate contextual metadata such as crop identification. The network architecture described at Section 3 is used as baseline.

Two different approaches are taken: A first approach that generates an independent model for each of the targeted crops and a second approach that develops a unique model multicrop for the entire dataset.

To train the single crop independent models, the dataset was split into the different crops (wheat, barley, corn and rape seed) and trained separately. This experiment measures the network ability to learn each individual visual task separately and thus, with no need of crop input information. Results for the baseline network over the full validation dataset are shown in Table 2.

For the second approach, the network is trained over the full dataset containing all crops, and serves as an estimation of the network capability of creating appropriate visual representations without crop information. Results for the baseline network over the full validation dataset are shown in Table 3.

The analysis of the results shows that the use of multi-crop models with higher number of images provides similar results as splitting the training dataset into the different crops. However, diseases with a lower number of images are benefited of the use of a multi-crop model. This is especially remarkable for the crops with lower number of images and variability. This shows that, under these training conditions, the extracted visual features and models are enriched by the use of a larger dataset with higher variability, superseding the performance of independent crop models.

4.3. Crop conditional Metadata and Image Convolutional Neural Network

Although experiments at 4.2 show slightly better performance using multi-crop approach, the network can still benefit from the additional contextual information of the crop being explicitly analyzed, as the visual similarities between diseases presenting similar symptoms in different crops reduce the performance of the network. This effect can be reduced by the use of crop species information as meta-data in the developed model. In this section we analyze the effect of including the crop species information in the model by the use of the three architectures detailed in 3.2. Results for the RESNET-MC-1 architecture are shown in Table 4, for the RESNET-MC-2 in Table 5 and RESNET-MC-3 in Table 6.

Table 7 summarizes the overall results for each of the analyzed topologies. We can appreciate that, when not using additional metadata or contextual information, results clearly show that the use of crop contextual metadata on a multi-crop approach super-seed any result obtained by each crop separately. This is caused by the fact that we take benefit from a larger dataset with much higher variability that is used by the CNN to extract more detailed and precise features and simultaneously, the contextual information derived from the crop ID information helps the network to discriminate among really similar diseases.

Besides this, the use of the proposed crop conditional RESNET-MC-1 architecture that integrates the Crop species information into a multi-crop model by concatenating the crop information on the embedding layer obtains the best performance. This might be caused by the fact that direct concatenation does not affect the gradient magnitude when training the network derivative towards the image CNN inner layers.

On the other hand, the multiplicative supression approaches (RESNET-MC-2 and RESNET-MC-3 topologies) failed to integrate the multiplicative suppression. Multiplicative suppression on the image embedding layer automatically scales the gradient magnitude by the suppression factor and thus, it can cause gradient inconsistencies and vanishing leading to poor convergence. This should be studied in further detail as future work.

The integration of the crop identification information by information concatenation as proposed in RESNET-MC-1 shown the best performance results with an average BAC of 0.98. This reduces the error rate from 7% to 2%.

5. Conclusions

In this work, we propose a crop conditional CNN architecture that seamlessly incorporates contextual meta-data consisting of the plant species identification. To validate the benefits of this approach we have generated a challenging dataset consisting of more than one hundred-thousand images taken by cell phone in real field wild conditions. This dataset containins almost equally distributed disease stages of seventeen diseases and five crops (wheat, barley, corn, rice and rape-seed).

When using the state of the art approach as baseline (Picon et al., 2018), our experiments prove that the use of a single model containing all crop and diseases achieves slightly better results than generating independent classification models per each crop. The use of independent single crop models showed an average BAC of 0.92, whereas the baseline multi-crop model showed an average BAC of 0.93.

When using the proposed crop conditional CNN architecture, we obtained richer and more robust shared visual features that yielded an average BAC of 0.98, which was superior to the other approaches and removes 71% of the classifier errors. This shows that t additional metadata can be easily included into deep learning models to allow categorical data-conditional classification which surpasses the performance obtained by other methods. The proposed method, simultaneously takes advantage on the visual information and variability from the full dataset without suffering from the effect of similar symptoms across crops.

In this work we have proven the benefits of large multi-crop approaches for plant disease characterization. This opens new research lines by encouraging the generation of large plant datasets and models that could easily take advantage of additional contextual information, few-shot or incremental learning techniques for new crops. Also the two proposed multiplicative suppression topologies will need additional focus and analysis.

Declaration of Competing Interest

Authors state that there is no conflict of interests on this work.

References

Ahmad, I.S., Reid, J.F., Paulsen, M.R., Sinclair, J.B., 1999. Color classifier for symptomatic soybean seeds using image processing. Plant Dis. 83, 320–327.

Alfarisy, A.A., Chen, Q., Guo, M., 2018. Deep learning based classification for paddy pests & diseases recognition. In: Proceedings of 2018 International Conference on Mathematics and Artificial Intelligence. ACM, pp. 21–25.

Amara, J., Bouaziz, B., Algergawy, A., et al., 2017. A deep learning-based approach for banana leaf diseases classification. In: BTW (Workshops), pp. 79–88.

Barbedo, J.G.A., 2013. Digital image processing techniques for detecting, quantifying and classifying plant diseases. SpringerPlus 2, 660.

Barbedo, J.G.A., 2016. A review on the main challenges in automatic plant disease identification based on visible range images. Biosyst. Eng. 144, 52–60.

Barré, P., Herzog, K., Höfle, R., Hullin, M.B., Töpfer, R., Steinhage, V., 2018. Automated phenotyping of epicuticular waxes of grapevine berries using light separation and convolutional neural networks. arXiv preprint arXiv:1807.07343.

Bereciartua, A., Picon, A., Galdran, A., Iriondo, P., 2015. Automatic 3d model-based method for liver segmentation in mri based on active contours and total variation minimization. Biomed. Signal Process. Control 20, 71–77.

Boutell, M., Luo, J., 2004. Bayesian fusion of camera metadata cues in semantic scene classification. In: Proceedings of the 2004 IEEE Computer Society Conference on Computer Vision and Pattern Recognition, 2004. CVPR 2004. IEEE. pp. II–II.

Boutell, M., Luo, J., 2005. Beyond pixels: exploiting camera metadata for photo classification. Pattern Recogn. 38, 935–946.

Brahimi, M., Arsenovic, M., Laraba, S., Sladojevic, S., Boukhalfa, K., Moussaoui, A., 2018. Deep learning for plant diseases: detection and saliency map visualisation. In: Human and Machine Learning. Springer, pp. 93–117.

Chambolle, A., 2004. An algorithm for total variation minimization and applications. J. Math. Imaging Vision 20, 89–97.

Chen, D.M., Baatz, G., Köser, K., Tsai, S.S., Vedantham, R., Pylvänäinen, T., Roimela, K., Chen, X., Bach, J., Pollefeys, M., et al., 2011. City-scale landmark identification on mobile devices. In: CVPR 2011, IEEE. pp. 737–744.

Cruz, A.C., El-Kereamy, A., Ampatzidis, Y., 2018. Vision-based grapevine pierce's disease

detection system using artificial intelligence. In: 2018 ASABE Annual International Meeting, American Society of Agricultural and Biological Engineers. p. 1.
Ferentinos, K.P., 2018. Deep learning models for plant disease detection and diagnosis. Comput. Electron. Agric. 145, 311–318.
Gulhane, V.A., Gurjar, A.A., 2011. Detection of diseases on cotton leaves and its possible diagnosis. Int. J. Image Process. (IJIP) 5, 590–598.
Gurjar, A.A., Gulhane, V.A., 2012. Disease detection on cotton leaves by eigenfeature regularization and extraction technique. Int. J. Electron. Commun. Soft Comput. Sci. Eng. (IJECSCSE) 1, 1.
Guru, D., Mallikarjuna, P., Manjunath, S., 2011. Segmentation and classification of tobacco seedling diseases. In: Proceedings of the Fourth Annual ACM Bangalore Conference. ACM, pp. 32.
He, K., Zhang, X., Ren, S., Sun, J., 2016. Deep residual learning for image recognition. In: Proceedings of the IEEE Conference on Computer Vision and Pattern Recognition, pp. 770–778.
Huang, G., Liu, Z., Van Der Maaten, L., Weinberger, K.Q., 2017. Densely connected convolutional networks. In: Proceedings of the IEEE Conference on Computer Vision and Pattern Recognition, pp. 4700–4708.
Huang, K.Y., 2012. Detection and classification of areca nuts with machine vision. Comput. Math. Appl. 64, 739–746.
Hughes, D., Salathé, M., et al., 2015. An open access repository of images on plant health to enable the development of mobile disease diagnostics. arXiv preprint arXiv:1511.08060.
Husin, Z.B., Shakaff, A.Y.B.M., Aziz, A.H.B.A., Farook, R.B.S.M., 2012. Feasibility study on plant chili disease detection using image processing techniques. In: 2012 Third International Conference on Intelligent Systems, Modelling and Simulation (ISMS). IEEE, pp. 291–296.
Jégou, S., Drozdzal, M., Vazquez, D., Romero, A., Bengio, Y., 2017. The one hundred layers tiramisu: Fully convolutional densenets for semantic segmentation. In: 2017 IEEE Conference on Computer Vision and Pattern Recognition Workshops (CVPRW), IEEE. pp. 1175–1183.
Johannes, A., Picon, A., Alvarez-Gila, A., Echazarra, J., Rodriguez-Vaamonde, S., Navajas, A.D., Ortiz-Barredo, A., 2017. Automatic plant disease diagnosis using mobile capture devices, applied on a wheat use case. Comput. Electron. Agric. 138, 200–209. http://www.sciencedirect.com/science/article/pii/S016816991631050X, doi:https://doi.org/10.1016/j.compag.2017.04.013.
Kamilaris, A., Prenafeta-Boldú, F., 2018. A review of the use of convolutional neural networks in agriculture. J. Agric. Sci. 1–11.
Kamilaris, A., Prenafeta-Boldú, F.X., 2018. Deep learning in agriculture: a survey. Comput. Electron. Agric. 147, 70–90.
Krizhevsky, A., Sutskever, I., Hinton, G.E., 2012. Imagenet classification with deep convolutional neural networks. In: Pereira, F., Burges, C.J.C., Bottou, L., Weinberger, K.Q. (Eds.), Advances in Neural Information Processing Systems 25. Curran Associates Inc., pp. 1097–1105. http://papers.nips.cc/paper/4824-imagenet-classification-with-deep-convolutional-neural-networks.pdf.
Kübler, E., 1994. Weizenanbau: 72 Tabellen. Ulmer.
Lu, J., Hu, J., Zhao, G., Mei, F., Zhang, C., 2017. An in-field automatic wheat disease diagnosis system. Comput. Electron. Agric. 142, 369–379.
Magarey, R., Fowler, G., Borchert, D., Sutton, T., Colunga-Garcia, M., Simpson, J., 2007. Nappfast: an internet system for the weather-based mapping of plant pathogens. Plant Dis. 91, 336–345.
Meunkaewjinda, A., Kumsawat, P., Attakitmongcol, K., Srikaew, A., 2008. Grape leaf disease detection from color imagery using hybrid intelligent system. In: 5th International Conference on Electrical Engineering/Electronics, Computer, Telecommunications and Information Technology, 2008. ECTI-CON 2008. IEEE. pp. 513–516.
Mirza, M., Osindero, S., 2014. Conditional generative adversarial nets. arXiv preprint arXiv:1411.1784.
Mohanty, S.P., Hughes, D.P., Salathé, M., 2016. Using deep learning for image-based plant disease detection. Front. Plant Sci. 7.
Oerke, E.C., 2006. Crop losses to pests. J. Agric. Sci. 144, 31–43.
Oerke, E.C., Gerhards, R., Menz, G., Sikora, R.A., 2010. Precision Crop Protection-The challenge and use of heterogeneity, vol. 5. Springer, pp. 5.
Omrani, E., Khoshnevisan, B., Shamshirband, S., Saboohi, H., Anuar, N.B., Nasir, M.H.N.M., 2014. Potential of radial basis function-based support vector regression for apple disease detection. Measurement 55, 512–519.
Paul, S., Sharma, R.D., 2016. Plant disease detection using image processing. Plant Disease 4.
Picon, A., Alvarez-Gila, A., Seitz, M., Ortiz-Barredo, A., Echazarra, J., Johannes, A., 2018. Deep convolutional neural networks for mobile capture device-based crop disease classification in the wild. Comput. Electron. Agric.
Picón, A., Rodríguez-Vaamonde, S., Jaén, J., Mocholi, J.A., García, D., Cadenas, A., 2012. A statistical recommendation model of mobile services based on contextual evidences. Expert Syst. Appl. 39, 647–653.
Pydipati, R., Burks, T., Lee, W., 2005. Statistical and neural network classifiers for citrus disease detection using machine vision. Trans. ASAE 48, 2007–2014.
Pydipati, R., Burks, T., Lee, W., 2006. Identification of citrus disease using color texture features and discriminant analysis. Comput. Electron. Agric. 52, 49–59.
Russakovsky, O., Deng, J., Su, H., Krause, J., Satheesh, S., Ma, S., Huang, Z., Karpathy, A., Khosla, A., Bernstein, M., Berg, A.C., Fei-Fei, L., 2015. ImageNet large scale visual recognition challenge. Int. J. Comput. Vision (IJCV) 115, 211–252. https://doi.org/10.1007/s11263-015-0816-y.
Sannakki, S.S., Rajpurohit, V.S., Nargund, V., Kulkarni, P., 2013. Diagnosis and classification of grape leaf diseases using neural networks. In: 2013 Fourth International Conference on Computing, Communications and Networking Technologies (ICCCNT). IEEE, pp. 1–5.
Shakoor, N., Lee, S., Mockler, T.C., 2017. High throughput phenotyping to accelerate crop breeding and monitoring of diseases in the field. Curr. Opin. Plant Biol. 38, 184–192.
Simonyan, K., Zisserman, A., 2014. Very deep convolutional networks for large-scale image recognition. arXiv preprint arXiv:1409.1556.
Siricharoen, P., Scotney, B., Morrow, P., Parr, G., 2016. A lightweight mobile system for crop disease diagnosis. In: International Conference Image Analysis and Recognition. Springer, pp. 783–791.
Sladojevic, S., Arsenovic, M., Anderla, A., Culibrk, D., Stefanovic, D., 2016. Deep neural networks based recognition of plant diseases by leaf image classification. Comput. Intell. Neurosci. 2016.
Stafford, J.V., 2000. Implementing precision agriculture in the 21st century. J. Agric. Eng. Res. 76, 267–275.
Szegedy, C., Vanhoucke, V., Ioffe, S., Shlens, J., Wojna, Z., 2016. Rethinking the inception architecture for computer vision. In: Proceedings of the IEEE Conference on Computer Vision and Pattern Recognition, pp. 2818–2826.
Tan, J.W., Chang, S.W., Kareem, S.B.A., Yap, H.J., Yong, K.T., 2018. Deep learning for plant species classification using leaf vein morphometric. IEEE/ACM Trans. Comput. Biol. Bioinformatics.
Venette, R.C., Kriticos, D.J., Magarey, R.D., Koch, F.H., Baker, R.H., Worner, S.P., Gómez Raboteaux, N.N., McKenney, D.W., Dobesberger, E.J., Yemshanov, D., et al., 2010. Pest risk maps for invasive alien species: a roadmap for improvement. Bioscience 60, 349–362.
Wang, H., Li, G., Ma, Z., Li, X., 2012. Image recognition of plant diseases based on principal component analysis and neural networks, in: 2012 Eighth International Conference on Natural Computation (ICNC), IEEE. pp. 246–251.
Xie, X., Zhang, X., He, B., Liang, D., Zhang, D., Huang, L., 2016. A system for diagnosis of wheat leaf diseases based on android smartphone, in: International Symposium on Optoelectronic Technology and Application 2016, International Society for Optics and Photonics. pp. 1015526–1015526.
Zhou, R., Kaneko, S., Tanaka, F., Kayamori, M., Shimizu, M., 2013. Early detection and continuous quantization of plant disease using template matching and support vector machine algorithms. In: 2013 First International Symposium on Computing and Networking (CANDAR). IEEE, pp. 300–304.